Toroidal cross capacitor for measuring the dielectric constant of gases

Thomas J. Buckley, Jean Hamelin,[a] and M. R. Moldover[b]
Physical and Chemical Properties Division, NIST, Gaithersburg, Maryland 20899-8380

(Received 1 February 2000; accepted for publication 27 March 2000)

We describe toroidal cross capacitors built to accurately measure the dielectric constant of gases. We tested the capacitors by measuring the dielectric polarizability of helium and argon at 7 and 50 °C at pressures up to 3 MPa. For helium, the results are consistent with the *ab initio* calculation of the molar polarizability and are limited by the uncertainties of the capacitance measurements. For argon, the results are consistent with the best previously published measurements of the polarizability and are limited by the uncertainties of the pressure measurements. Lessons learned are provided. [S0034-6748(00)02407-2]

I. INTRODUCTION

Often, precise capacitance measurements are combined with the Clausius–Mossotti relation to determine the density of gases $\rho(p,T)$ as a function of the temperature and the pressure and also to detect the onset of phase separation. Conventionally, capacitors designed for these purposes[1–3] have coaxial, guarded electrodes. One advantage of the coaxial configuration is that the capacitance is insensitive, in the first order, to small radial and longitudinal translations of the inner electrode with respect to the outer electrode. The coaxial designs cited have a second advantage; namely, the solid insulators supporting the electrodes are located in regions of negligible electric field. Thus, the dielectric properties of the insulators do not influence the measurements of the dielectric properties of the gases. In the present work, we used a cross capacitor in place of a coaxial capacitor. Cross capacitors have the advantages of the coaxial designs and an additional advantage; namely, they are insensitive, in the first order, to thin dielectric films on the electrode surfaces.[4,5] Such films might be oxide layers, adsorbed water, pump oil, etc. The insensitivity of cross capacitors to surface films was essential for their use as a standard of electrical phase angle[5] and it will be important whenever the dielectric constant of gases must be measured with the highest possible accuracy. Highly accurate measurements of the dielectric constant of helium were used to determine the thermodynamic temperature in the range 4.2–27 K.[6] We are planning even more accurate measurements of the dielectric constant of helium at 273.16 K for use as a standard of pressure in the range 0.5–5 MPa.[7]

We manufactured two nearly identical cross capacitors and used them with commercially manufactured instruments to measure the dielectric constants of helium and argon at 7 and 50 °C and at pressures up to 3 MPa. The resulting value of the molar polarizability A_ϵ of helium agrees, within experimental error, with the theoretical value. This demonstrated that the cross capacitors deformed as predicted when they were compressed by the helium. The predicted performance is confirmed by the good agreement of our argon results with measurements made in other laboratories. Finally, while evacuated, the temperature dependence of each cross capacitor was close to that predicted from the dimensions and thermal expansion of its sapphire and superinvar components. Taken together, these test results demonstrate that cross capacitors may be used to make very accurate measurements of the dielectric constant of gases.

II. CROSS CAPACITORS

A. Infinitely long cylinders

Figure 1 is the cross section of an idealized cross capacitor comprised of four infinitely long, cylindrical conductors separated by infinitesimal gaps and forming a closed curve of arbitrary cross section. The importance of such structures to metrology was pointed out by Thompson and Lampard.[8] Lampard proved[4] that the capacitances per unit length C_1 and C_2 between opposing pairs of conductors obey the relationship

$$\exp(-\pi C_1/\epsilon_0)+\exp(-\pi C_2/\epsilon_0)=1, \tag{1}$$

where the electric constant (the electric permittivity of vacuum) $\epsilon_0=10^7/[4\pi c_0^2/(\mathrm{m\,s^{-1}})^2]\mathrm{F\,m^{-1}}$ is known exactly using the defined speed of light $c_0\equiv 299\,792\,458\,\mathrm{m\,s^{-1}}$. Equation (1) is remarkable because it is true regardless of the shapes of the cylindrical conductors' cross sections. Equation (1) is particularly useful when $C_1\approx C_2$. For this case one defines the mean capacitance $C_x\equiv(C_1+C_2)/2$ as ''the'' cross capacitance. Using the definition $\Delta C\equiv(C_1-C_2)$, one then finds

$$\begin{aligned} C_x &= \frac{\epsilon_0 \ln 2}{\pi}\left[1+\frac{\ln 2}{8}(\Delta C/C_x)^2+\cdots\right] \\ &= 1.953\,549\ldots[1+0.086\,64\ldots(\Delta C/C_x)^2 \\ &\quad +\ldots]pF/m, \end{aligned} \tag{2}$$

which shows that C_x depends upon $\Delta C/C_x$ in the second order. This second-order dependence allows one to design

[a]Present address: Institut de Recherche sur l'Hydrogène, Université du Québec à Trois-Rivières, 3351 Boul. Des Forges, C.P. 500, Trois-Rivières, Québec, Canada G9A 5H7.
[b]Author to whom correspondence should be addressed; electronic mail: michael.moldover@nist.gov

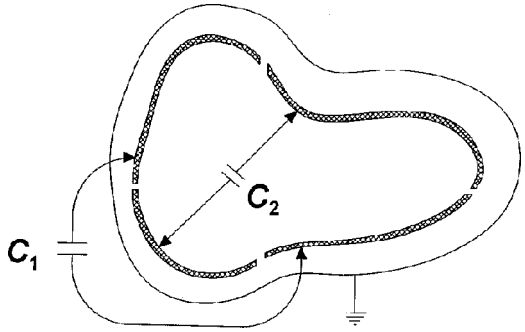

FIG. 1. Thompson–Lampard cross capacitor. The shaded curves represent the cross section of four infinitely long cylindrical conductors separated by narrow gaps.

cross capacitors that are remarkably insensitive to details of their construction. For many years, this insensitivity was exploited by national standards laboratories that used long, evacuated, cylindrical cross capacitors as impedance standards to realize the ohm.[9] Despite this history, we have not found published accounts of the use of cross capacitors to measure the dielectric constants of gases. Two reasons for this are implicit in Eq. (2). First, only very small values of C_x are available for capacitors of modest lengths; thus, the applications of cross capacitors demand very high-quality capacitance bridges. Second, two measurements of capacitance are required to determine each value of C_x. Thus, measuring C_x requires more time and more equipment (well-shielded switches between the bridge and the capacitor) than conventional capacitance measurements.

For accurately measuring the dielectric constants of gases, a cross capacitor must be stable, compact enough to fit within a pressure vessel (which itself must fit within a thermostat), and constructed from materials that will not contaminate pure gases. It is also essential that the deformation of the cross capacitor under hydrostatic pressure be predictable. It is desirable, but not essential, that the cross capacitors have small coefficients of thermal expansion and that they are simple to construct. The requirement for compactness led us to consider toroidal cross capacitors.

B. Toroidal cross capacitors

Toroidal cross capacitors are formed by four conducting tori separated by small gaps. The cross sections of the tori, like those of the Thompson–Lampard cylinders, are arbitrary. Indeed, the Thompson–Lampard cross capacitor is a special toroidal cross capacitor where the major radii of the tori are infinite.[10] In Fig. 2, we consider an idealized toroidal cross capacitor with a square cross section with height (h) = width (w) = d. Shields[5] used such a capacitor as a standard for the absolute measurement of the loss angle of conventional capacitors and also to verify that cross capacitors are insensitive to dielectric films on their electrodes.[11] Figure 2 shows four gaps of thickness s separating the vertical electrodes from the horizontal ones. For this design, the dependencies of the cross capacitance on the size of the insulating gaps and on the average radii r of the tori are:[12]

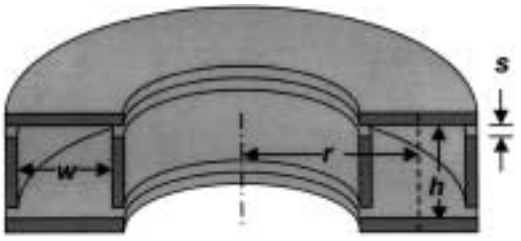

FIG. 2. Schematic cross section of a toroidal cross capacitor with a nearly square cross section. For the prototype capacitors, the dimensions were: $r \approx 50$ mm, $w \approx 10$ mm, $h \approx 9.5$ mm, and $s \approx 0.15$ mm.

$$C_x = 2 \ln 2 r \epsilon_0 \epsilon f(d/r, s/d),$$
$$f(d/r, s/d) = 1 - 0.040\,42(d/r)^2 - 0.0017(s/d)^2 + \cdots. \quad (3)$$

Equation (3) demonstrates that C_x depends on the thicknesses of the gaps in the second order $(s/d)^2$ and also on the curvature of the tori in the second order $(d/r)^2$. In our prototype capacitors (Fig. 3), $r \approx 50$ mm, $d \approx 10$ mm, and $s \approx 0.15$ mm. The dependence of C_x on the thicknesses of the gaps is very small: $(\partial C_x/\partial s)/C_x = -5 \times 10^{-5}/d$. The corresponding derivative for a conventional, parallel-plate capacitor with an insulating gap of thickness s is much larger: $(\partial C_x/\partial s)/C_x = -1/s$.

Our prototype toroidal cross capacitors were designed to have square cross sections; however, they were slightly rectangular. When the deviation $\delta \equiv 1 - (\text{height})/(\text{width})$ of the cross section from a square is small, the cross capacitance is second order in the deviation:[12]

$$C_x = 2 \ln 2 r \epsilon_0 \epsilon (1 + 3.454\delta^2 + \cdots). \quad (4)$$

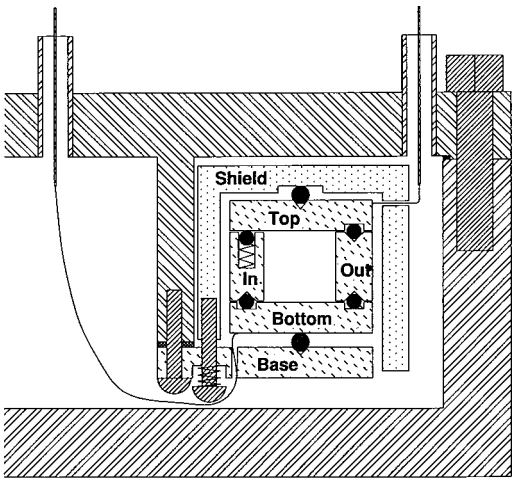

FIG. 3. Schematic cross section of prototype cross capacitor inside its pressure vessel. The insulating sapphire balls are represented by solid circles. The hatched areas indicate metal components. The pressure vessel was stainless steel; the shield was aluminum; and the electrodes and the base were superinvar. A spring embedded within the ''In'' electrode presses a sapphire ball against the ''Top'' electrode. Another spring around a bolt holds the shield against the base. Electrical leads from the top and bottom electrodes to feedthroughs are indicated.

C. Prototype capacitors

We assembled two nearly identical toroidal cross capacitors and installed them in separate, nearly identical pressure vessels. For future reference, they are identified as Nos. 1 and 2. The pair of cross capacitors are suitable for using the methods of Burnett[13] and of Buckingham, Cole, and Sutter,[14] to measure the density virial coefficient $B(T)$ and the dielectric virial coefficient $b(T)$, as defined in Eqs. (7) and (8) in Sec. IV B below. When these methods are used, one pressure vessel is evacuated and the second is filled with the test gas. The pressure and both capacitances are measured. The test gas is allowed to expand into the second capacitor and the pressure and capacitances are measured again. Then, the roles of the filled and evacuated capacitors are interchanged. The data can be used to eliminate the first-order effects of the deformation of the pressure vessel while determining the properties of the test gas.

As shown in Fig. 3, each prototype capacitor was comprised of four toroidal electrodes that were insulated from each other by sapphire balls. To facilitate discussion, we refer to the electrodes as inner (I), outer (O), top (T), and bottom (B). We denote the capacitance between the top and the bottom electrodes as C_{TB}, etc. All four electrodes were right circular cylinders; the top and bottom electrodes were disklike and the inner and outer electrodes were tubelike. These simple shapes facilitate using conventional machine-shop techniques to fabricate and polish the metal electrodes. The electrodes were bored out of $\frac{1}{2}$-in.-thick superinvar plate stock purchased from Robin Materials Inc.[15]

Sapphire balls, 2 mm in diameter, were used to insulate the electrodes from each other. The electrodes were insulated from the aluminum shield surrounding them and from the superinvar base by sapphire balls 2.5 mm in diameter. For the first capacitor, C_1, the balls and electrodes were assembled in a stable nearly kinematic structure. Three radial ''V'' grooves were electrodischarge machined into the top and bottom electrodes and three mating cavities were electrodischarge machined into the inner and outer electrodes. Each cavity had three plane surfaces meeting at right angles in the shape of the corner of a cube. Thus, each ball contacted the top and the bottom electrodes at two points and the inner and outer electrodes at three points. For expediency, electrodischarge-machined cavities were not used in the second capacitor, C_2. Instead, conical cavities were made in the inner and outer electrodes using a center drill. Thus, the balls contacted these electrodes along arcs.

The thicknesses of the gaps between the electrodes were designed to be small to minimize the dependence of the cross capacitance upon the dielectric properties of the sapphire balls. (When C_{TB} and C_{IO} are measured, the electric fields decay exponentially with distance into the gaps.) The thicknesses of the gaps were estimated from measurements of the capacitances between pairs of electrodes while all the other conductors were grounded. For C_1, the thicknesses ranged from 0.14 to 0.17 mm; for C_2, the thicknesses ranged from 0.13 to 0.18 mm.

In an early version of this apparatus, the capacitors were held together simply by the weight of the top electrode. This was unsatisfactory because the capacitances fluctuated in response to ambient vibrations. The present design uses three springs to apply a modest force between the shield and the top electrode. In turn, the top electrode holds the outer and bottom electrodes against the base. Three other springs embedded in the inner electrode press balls against the top electrode.

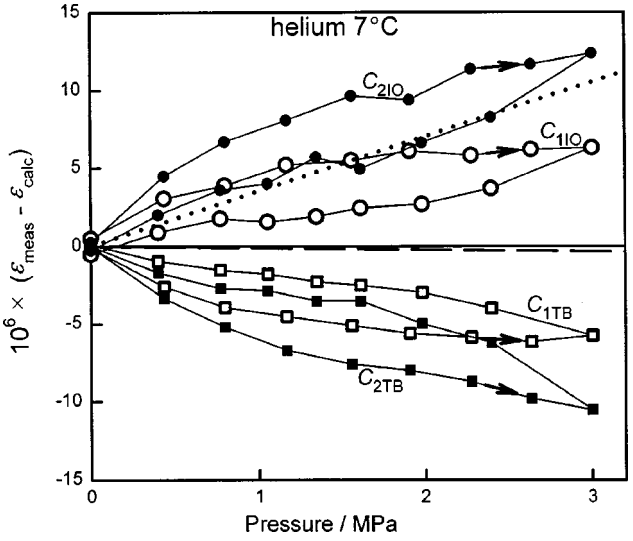

FIG. 4. Deviations of measured values of the dielectric constant of helium from the calculated values. Four data sets for ϵ_{meas} are plotted; each set is labeled by the pair of electrodes used. The arrows indicate the progression of the data as the pressure was raised in steps to 3 MPa and then lowered in steps. The calculations for ϵ_{calc} used the *ab initio* values of the molar polarizability A_ϵ and density virial coefficient $B(T)$. The calculations included the effects of the measured compressibility α_P of superinvar (dotted line) and the dielectric virial coefficient b (dashed line) (see Ref. 23).

Equation (2) was obtained by considering only the electric fields enclosed by the four electrodes. By assumption, the fields outside the electrodes made negligible contributions to the cross capacitance because a grounded shield closely surrounded these electrodes (Fig. 1). The prototype apparatus shown in Fig. 3 approximated this situation very well by surrounding the four superinvar electrodes with a grounded aluminum shield. In an earlier version of this apparatus, we relied upon the pressure vessel and the cylindrical plate supporting the electrodes to serve as the grounded shield. This arrangement was unsatisfactory because the shield was too far from the electrodes. Then, C_{TB} and C_{IO} had undesirable dependencies upon the proximity of the vessel to the electrodes which varied as the vessel deformed when it was filled with gas at a high pressure. The aluminum shield greatly reduced the pressure dependence of C_{TB} and C_{IO}. However, the remaining pressure dependence of C_{TB} and C_{IO} implied by Fig. 4 indicates that more improvement may be possible.

D. Asymmetric cross capacitors

After assembling both cross capacitors, we found that $C_{\mathrm{TB}} \approx 0.72$ pF and $C_{\mathrm{IO}} \approx 0.52$ pF. This large asymmetry was not intentional. The superinvar electrodes had been cut from the plate stock and then heat treated. During heat treatment, the electrodes warped more than we anticipated and they had

to be re-machined. The additional machining reduced the heights of the inner and outer electrodes and the cross section became a rectangle with $\delta \equiv 1 - (\text{height})/(\text{width}) \approx 0.05$. This value of δ explains nearly all the differences between C_{TB} and C_{IO} and their mean, 0.62 pF. Furthermore, δ is sufficiently large that its temperature and pressure dependencies would have appeared in the data for C_x if we had used the symmetrical definition $C_x \equiv (C_1 + C_2)/2$. Instead, following Makow and Campbell's suggestion,[16] we defined C_x by

$$C_x \equiv wC_{TB} + (1-w)C_{IO}, \tag{5}$$

where the value $w = 0.45$ was chosen to insure that $\partial C_x/\partial \delta = 0$ at $\delta = 0.05$.

E. Deformation of the capacitors with temperature and pressure

With the asymmetric weighting of C_{TB} and C_{IO}, the cross capacitance depends, in the first order, only on the average major radius $r \approx 50$ mm of the tori. This average is determined solely by the inner radius of the outer electrode and the outer radius of the inner electrode. Both electrodes were made from a single superinvar plate and both were subject to small forces from springs, gravity, electric fields, and buoyancy. Thus, we expected that the temperature and pressure dependencies of r and of C_x would be those of superinvar alone.

The dielectric constant ϵ was determined from the ratio $C_x(p)/C_x(0)$, where $C_x(p)$ was the cross capacitance of each toroidal cross capacitor immersed in a test gas at a pressure p and $C_x(0)$ was the cross capacitance of the same capacitor when evacuated. We assume that the radii of the superinvar cylinders (and C_x) decreased as linear functions of pressure characterized by a coefficient α_p. Upon including this effect, the expression for ϵ is

$$\epsilon(p) = \frac{C_x(p)}{C_x(0)}(1 - \alpha_p p). \tag{6}$$

We used the value $\alpha_p = -3.15 \times 10^{-12}\ \text{N}^{-1}\,\text{m}^2$ which is $\frac{1}{3}$ of the average value of the reciprocal of the adiabatic bulk modulus of elasticity measured for three superinvar samples. To measure α_p, small rectangular parallelpipeds were cut out of the superinvar plates when they were received from the manufacturer. Migliori (Los Alamos National Laboratory) used the well-established technique[17] of resonant ultrasound spectroscopy (RUS) to determine the adiabatic bulk modulus. His result was $(1.06 \pm 0.04) \times 10^{11}\ \text{N m}^{-2}$, where the standard uncertainty was calculated using the different results for the three samples. For superinvar, the correction from the adiabatic bulk modulus provided by RUS to the isothermal bulk modulus required for α_p is very small. Three similar parallelpipeds were cut out of the electrodes after they had been heat treated. However, the quality factors of the ultrasonic resonances in these samples were too low to use RUS.

In assessing the performance of the individual capacitances C_{TB} and C_{IO}, we must consider the properties of sapphire as well as those of superinvar. The thicknesses of the gaps s are determined by the difference between approximately 1.28 mm of sapphire and 1.13 mm of superinvar. (The scale for these dimensions is set by the diameters of the sapphire balls. The specific values 1.28 and 1.13 mm depend upon the angles of the ''V'' grooves and tetrahedral or conical cavities.) Thus, when assessing the effects of temperature and pressure upon the prototype shown in Fig. 3, the small values of $(\partial C_x/\partial s)/C_x$ must be multiplied by a factor on the order of (radius of ball)/s. The heights of the cross capacitors were determined by the sum of approximately 2.6 mm of sapphire and 6.9 mm of superinvar. The widths of the cross capacitors were determined by approximately 10 mm of superinvar. From these dimensions and published data, we estimated the thermal expansions to be: $(dC_{TB}/dT)/C_{TB} = -4.5 \times 10^{-6}\ \text{K}^{-1}$ and $(dC_{IO}/dT)/C_{IO} = 4.8 \times 10^{-6}\ \text{K}^{-1}$. When these estimates are used to estimate the thermal expansion of the weighted cross capacitance, the result is $(dC_x/dT)/C_x = -0.08 \times 10^{-6}\ \text{K}^{-1}$.

III. PERFORMANCE TESTS

To test the performance of the cross capacitors, we studied their behavior when evacuated and we used them to measure the dielectric constants of helium and argon at pressures up to 3 MPa at two temperatures: 7 and 50 °C. Here, we describe the instruments used, the procedures, and finally, the results.

A. Instruments

All the capacitance measurements were made using an automated bridge (model AH-2500A, option E) manufactured by Andeen-Hagerling Inc.[15] Coaxial cables with grounded shields led from the bridge to an array of coaxial relays (model 7102, Matrix Systems, Inc.[15]). During each capacitance measurement, all of the conductors were grounded via the relays except for the two electrodes that were connected to the bridge.

For the performance tests, both pressure vessels were placed in the same multishell thermostat in an insulated air bath. The temperature of one capacitor was measured with a capsule-type standard platinum resistance thermometer. This thermometer had been calibrated on ITS-90 and was embedded in a metal block fastened to the bottom of the pressure vessel surrounding C_1. A three-junction thermopile was used to measure the difference between the temperatures of the two pressure vessels. When the temperature was constant, we estimate that the uncertainties of the temperatures of the capacitors were less than 10 mK; thus, they are neglected here.

Both pressure vessels were connected to the same gas manifold at all times. Above 3 MPa, one of the pressure vessels leaked at its metal O-ring seal; this limited the maximum pressure of the data to 3 MPa. The pressure of the test gas was measured using a model RPM1 sensor manufactured by DH Instruments.[15] The sensor had a full-scale range of 6.894 MPa. The manufacturer's specification includes: ''Absolute Accuracy: $\pm$(0.01% F.S.+0.005% of reading) for 90 days.'' At the conclusion of the test measurements, the pressure sensor was calibrated with respect to a piston gage. Near 3 MPa, the sensor's indication was 210 Pa less than that of

the standard; near 2.2 MPa, its indication was 90 Pa less than the standard, and near 0.9 MPa its indication was 40 Pa greater than the standard. We also monitored the zero indication of the pressure sensor. The absolute value of the zero indication changed an average of 22 Pa during the intervals of one to three days that were used to measure the polarizability along the isotherms. The calibration data and the zero indications were consistent with the manufacturer's specifications. When analyzing our data for A_ϵ, we used the calibration data to correct the indications of the pressure sensor and we weighted the data for the uncertainty of the pressure by the expression $[(5\times10^{-5}p)^2+(\sqrt{2}\times 22\ \mathrm{Pa})^2]^{1/2}$.

B. Procedures

Both the helium and the argon were purchased from Matheson Gas Products[15] and specified by the manufacturer to be ''99.9999% minimum purity'' by volume. The manufacturer specified that the water content of the helium was $<0.2\times10^{-6}$ by volume and that the water content of the argon was $<1\times10^{-6}$ by volume.

Before measuring each isotherm, the capacitors were thoroughly flushed with the test gases by repeatedly filling them to a high pressure and then evacuating them with a trapped, rotary vacuum pump. For the measurements with the test gases, the pressure was increased from zero to 3 MPa in 6 to 8 equally sized steps and then reduced back to zero in similar steps. The adiabatic compression or expansion of the test gas within the pressure vessels caused significant temperature changes. Following each pressure step, the capacitances, temperatures, and the pressure were monitored during an interval of 3–5 h as the temperature relaxed towards the set point of the thermostat. During the last 10 min of each interval, the capacitance data were averaged and recorded for analysis.

IV. RESULTS

A. Results under vacuum

On 26 occasions during an 84-day-long interval, the cross capacitances were measured while they were evacuated. During the first 10 days, the capacitors were near 25 °C; during the next 57 days, they were near 50 °C; and during the final 17 days, they were in the range 7 °C to 10 °C. Between the vacuum measurements, the capacitors were filled with test gases at pressure up to 3 MPa. The vacuum results were fitted to linear functions of the temperature and of the elapsed time. These fits determined the average coefficients of thermal expansion and tested for creep.

The thermal expansion averaged over the interval 7 °C to 50 °C, $\langle\alpha_T\rangle=\langle(dC_x/dT)/C_x\rangle$, was $(5.4\pm0.4)\times10^{-8}$ K^{-1} for C_{1x} and $(24.6\pm0.3)\times10^{-8}$ K^{-1} for C_{2x}. Both values of $\langle\alpha_T\rangle$ are small and positive. If the thermal expansion were that of superinvar alone, we would have expected a result such as $\langle\alpha_T\rangle\approx-11\times10^{-8}$ K^{-1} from the data of Jacobs, Johnston, and Schway,[18] or $\langle\alpha_T\rangle\approx-16\times10^{-8}$ K^{-1} from the data of Berthold, Jacobs, and Norton.[19] After including the sapphire in the model (Sec. III E), we expected $\langle\alpha_T\rangle\approx-8\times10^{-8}$ K^{-1} using the data of Jacobs, Johnston, and Schway.[20] The differences between the measured and the expected values of $\langle\alpha_T\rangle$ are very small; indeed, they are less than one part per million per kelvin.

In Sec. II E, we considered the thermal expansions of the component capacitances C_{TB} and C_{IO}. The estimate $\langle\alpha_T\rangle_{\mathrm{TB}}\equiv(dC_{\mathrm{TB}}/dT)/C_{\mathrm{TB}}=-4.5\times10^{-6}$ K^{-1} can be compared with the results $\langle\alpha_T\rangle_{1\mathrm{TB}}=-15.0\times10^{-6}$ K^{-1} and $\langle\alpha_T\rangle_{2\mathrm{TB}}=-9.1\times10^{-6}$ K^{-1}. As expected, the thermal expansions of $C_{1\mathrm{TB}}$ and $C_{2\mathrm{TB}}$ were negative; however, their magnitudes were two to three times larger than expected. Similarly, the estimate $\langle\alpha_T\rangle_{\mathrm{IO}}=4.8\times10^{-6}$ K^{-1} can be compared with the results $\langle\alpha_T\rangle_{1\mathrm{IO}}=16.9\times10^{-6}$ K^{-1} and $\langle\alpha_T\rangle_{2\mathrm{IO}}=10.7\times10^{-6}$ K^{-1}. As expected, the thermal expansions of $C_{1\mathrm{IO}}$ and $C_{2\mathrm{IO}}$ were positive; however, they also were two to three times larger than expected. We cannot explain the discrepancies in the magnitudes; however, as indicated in the preceding paragraph, the cross capacitance compensated for the unexpected temperature dependencies of the component capacitances C_{TB} and C_{IO}.

Averaged over 84 days, the time dependence was $(dC_x/d\mathrm{time})/C_x=(0.74\pm0.89)\times10^{-6}$ year^{-1} for C_{1x} and $(-8.50\pm0.69)\times10^{-6}$ year^{-1} for C_{2x}. An additional uncertainty of 0.5×10^{-6} year^{-1} should be added in quadrature to the uncertainties of these time dependencies, to allow for the drift of the capacitance bridge and its internal standard, according to the manufacturer's specifications. We have no certain explanation for the comparatively large time dependence of the cross capacitance C_{2x}. Nevertheless, this time dependence was not large enough to cause difficulties when measuring the dielectric constants of helium and argon. The time dependencies may be compared with the observation made by Jacobs, Johnston, and Schway:[18] ''We were surprised to find that at 60 °C the temporal stability of the Super-Invar sample (labeled *S*), whose 27 °C growth rate we previously determined at <0.001 ppm/year, had degenerated to rates no better than can be had with the best commercial Invar (1.1–1.5 ppm/year).''

The standard uncertainty of the residuals from fitting the measurements of C_x in vacuum was 0.17 aF. This is an upper bound to the standard uncertainty of the capacitance measurements. (If the assumptions of *linear* time and temperature dependencies were dropped, the residuals would decrease slightly.) The dielectric constant is computed from the ratio of two measurements of C_x; thus, one expects that the standard uncertainty of ϵ will be $\sqrt{2}\times0.17\,aF/C_x=3.8\times10^{-7}$, or smaller. This uncertainty contributes to the relative uncertainty of the molar polarizability $u_r(A_\epsilon)=3.8\times10^{-7}/(\epsilon-1)$. [For argon at 3 MPa and 7 °C, $\epsilon\approx1.016$ and $u_r(A_\epsilon)\approx2.4\times10^{-5}$; for helium under the same conditions, $\epsilon\approx1.002$ and $u_r(A_\epsilon)\approx1.9\times10^{-4}$.] For helium, the uncertainty of the capacitance measurements is the only important contribution to the uncertainty of the dielectric constant and the molar polarizability computed from it.

B. Results with helium

For helium, the experimental results were compared with the theoretical values of the capacitance that we obtained by

numerically eliminating the density from the virial expansion for the pressure

$$p=\rho RT[1+B(T)\rho+C(T)\rho^2+\ldots], \tag{7}$$

and the virial expansion for the dielectric polarizability P_ϵ:

$$P_\epsilon=\frac{\epsilon-1}{\epsilon+2}\frac{1}{\rho}=A_\epsilon[1+b(T)\rho+c(T)\rho^2+\ldots]. \tag{8}$$

Here, $B(T)$ and $C(T)$ are the density virial coefficients, $b(T)$ and $c(T)$ are the dielectric virial coefficients, A_ϵ is the molar polarizability of helium, and R is the molar gas constant. In this test, we used the theoretical value of A_ϵ cited by Luther, Grohmann, and Fellmuth[6] and the theoretical values of $B(T)$ from Hurly and Moldover[21] [$B(7\,^\circ\text{C})=11.878\ \text{cm}^3\,\text{mol}^{-1}$ and $B(50\,^\circ\text{C})=11.702\ \text{cm}^3\,\text{mol}^{-1}$]. From the measurements of Kell, McLaurin, and Whalley[22] and Huot and Bose,[23] we know that the terms $C(T)\rho^2$, $b(T)\rho$, and $c(T)\rho^2$ in Eqs. (7) and (8) are very small for helium below 3 MPa.

Figure 4 displays the deviations of the measured dielectric constants ϵ_{meas} from the values calculated ϵ_{calc} for helium at 7 °C. For Fig. 4, the capacitance data from the pairs of electrodes $C_{1\text{IO}}$, $C_{2\text{IO}}$, $C_{1\text{TB}}$, and $C_{2\text{TB}}$ were treated as if they were acquired from four, independent capacitors. From the four pairs of electrodes, we deduced four values of ϵ_{meas} using Eq. (6) and they are plotted in Fig. 4. Figure 4 demonstrates that C_{IO} changed more with pressure than predicted and that C_{TB} changed less than predicted. Perhaps, as the pressure was raised, the aspect ratio h/w increased. At 3 MPa, this interpretation requires a relative displacement of the top and bottom electrodes that is approximately 30 nm larger than the relative displacement of the inner and outer electrodes.

Figure 4 also shows that the data taken as the pressure increased are inconsistent with the data taken as the pressure decreased. Typically, at the times the data were recorded, the temperature of the capacitors was 0.1 K higher for the pressure-increasing data than for the pressure-decreasing data. The measured thermal expansions ($\alpha_T\times 0.1$ K) are too small to directly explain the hysteresis observed.

The dotted line in Fig. 4 shows the effect of the compressibility of the capacitor calculated using Eq. (6). If we had not accounted for the compressibility, the average of the experimental values of dielectric constants would have been much smaller than the theoretical values. The dashed line in Fig. 4 shows the effect of the dielectric virial coefficient $b(T)$ on the calculation. This effect is smaller than the random variations in ϵ_{meas}. Thus, these instruments cannot be used to determine $b(T)$, unless the maximum pressure is greatly increased and/or the uncertainty of the capacitance measurements is reduced.

The same capacitance measurements that were used to construct Fig. 4 are replotted in the lower panel of Fig. 5. However, in Fig. 5, ϵ_{meas} was computed from the weighted cross capacitances $C_{1x}\equiv 0.45C_{1\text{TB}}+0.55C_{1\text{IO}}$ and $C_{2x}\equiv 0.45C_{2\text{TB}}+0.55C_{2\text{IO}}$. The values of ϵ_{meas} from both cross capacitors at both temperatures are all within 10^{-6} of the theoretical values. At 7 °C, the standard deviations of $10^6\times(\epsilon_{\text{meas}}-\epsilon_{\text{calc}})$ are 0.15 and 0.21 for the data from C_{1x} and C_{2x}, respectively; at 50 °C, the corresponding standard deviations are 0.29 and 0.34. These standard deviations are slightly less than the value 0.38 obtained from the vacuum measurements that extended over 84 days and 43 °C. From these results, we assert, for helium, ϵ_{meas} obtained from the cross capacitances agrees with ϵ_{calc} within the uncertainty attainable from the capacitance bridge.

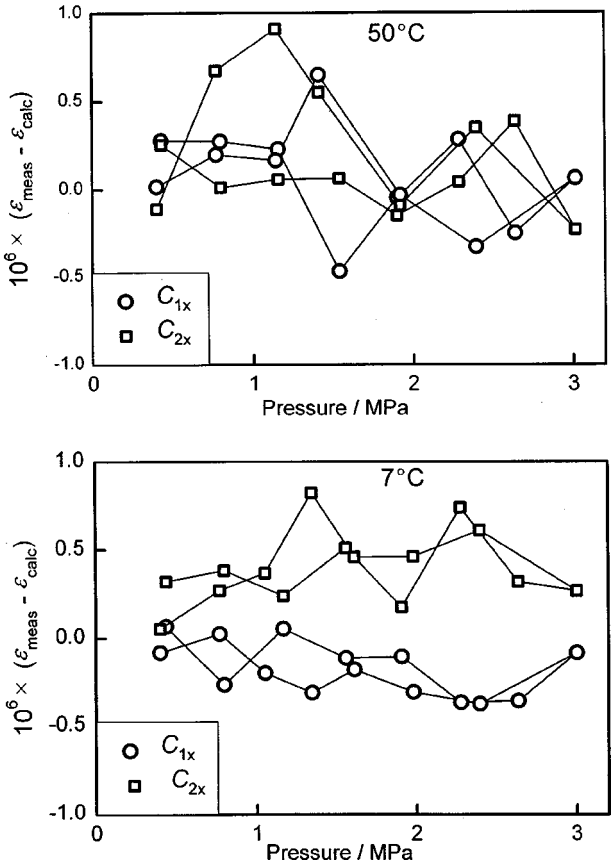

FIG. 5. Deviations of measured values of the dielectric constant of helium from the calculated values on two isotherms. For these figures, ϵ_{meas} was deduced from the asymmetric cross capacitances $C_{1x}\equiv 0.45C_{1\text{TB}}+0.55C_{1\text{IO}}$ and $C_{2x}\equiv 0.45C_{2\text{TB}}+0.55C_{2\text{IO}}$. Because the cross capacitor compensates for relative displacements its component electrodes, we could expand the ordinate of Fig. 4 by a factor of 15 and plot the same data.

The effect of the hydrostatic compression of superinvar was 40 times the mean standard deviation ($\epsilon_{\text{meas}}-\epsilon_{\text{calc}}$); thus, the good agreement of ϵ_{meas} and ϵ_{calc} would not have been obtained if the compression of the superinvar had been overlooked.

Taken together, Figs. 4 and 5 comprise a graphic demonstration of the effectiveness of the cross capacitance concepts in compensating for the relative motion of the electrodes, even in the present case, where we do not have a detailed explanation for the relative motion of the components of the capacitors.

We recall that this analysis of the helium data used the *ab initio* values for A_ϵ and $B(T)$. This is rarely done in assessing the reliability of measurements of thermophysical properties. Conventionally, new results are compared with prior measurements. To make a conventional comparison, we fitted $[(\epsilon-1)/(\epsilon+2)]\times[RT/p]$ to linear functions of the pressure p. In such linear fits, the intercepts at $p=0$ are values of A_ϵ and the slopes are values of $[b(T)$

TABLE I. Molar polarizability of helium and argon.

$A_\epsilon/(\mathrm{cm}^3\ \mathrm{mol}^{-1})$	Temperature	Reference
	Helium	
0.517 253 ± 0.000 010	[a]	6
0.517 47 ± 0.000 20	7 °C, 50 °C	This work
0.5196 ± 0.0002	50 °C	23
0.519 ± 0.001	40 °C	24
	Argon	
4.1397 ± 0.0006	50 °C	23
4.146 ± 0.003	25 °C	26
4.140 ± 0.003	7 °C to 57 °C	27
4.140 78 ± 0.000 39	7 °C, 50 °C	This work

[a]The *ab initio* value is independent of temperature.

$-B(T)]RT/A_\epsilon$. The data were weighted by $3.8\times10^{-7}/(\epsilon-1)$, the uncertainty of ϵ_{meas} estimated from the vacuum measurements. Four fits were carried out; two used the asymmetric cross capacitor data from C_{1x} and C_{2x} at 7 °C; two used the data at 50 °C. As expected, the values of A_ϵ at 7 and 50 °C were identical, within the uncertainties. The average of all four values of A_ϵ and their standard uncertainty appear in Table I. The excellent agreement between the fitted values of A_ϵ and the *ab initio* value is not surprising after considering Fig. 5.

Our results and the *ab initio* value of A_ϵ are slightly smaller than two previous measurements.[23,24] We have no sure explanation for this. Both our measurements and the *ab initio* calculations will be improved.[25]

C. Results with argon

For argon, the *ab initio* values of A_ϵ and $B(T)$ are not sufficiently accurate to critically test the cross capacitors; thus, we only compare the present data with experimental results from the literature. We corrected our cross capacitance data for the hydrostatic compression of the capacitor via Eq. (6) and computed values of $[(\epsilon-1)/(\epsilon+2)]\times[RT/p]$ and fitted them to polynomial functions of p. Quadratic polynomials of p were needed to fit the argon data within their uncertainty. (Quadratic terms were not needed for helium because the pressure dependence of ϵ of helium is eight times smaller than that of argon.) Figure 6 displays the argon data, the fitted polynomials, and the deviations of the data from the polynomials. When fitting the argon data, we weighted them by the sum in quadrature of relative uncertainties of the dielectric constant measurements $u_r(\epsilon)=3.8\times10^{-7}/(\epsilon-1)$ and the relative uncertainties of the pressure measurements $u_r(p)=[(5\times10^{-5})^2+(\sqrt{2}\times22\ \mathrm{Pa}/p)^2]^{1/2}$. The weights are shown as dotted curves in Fig. 6.

The fits resulted in two values of A_ϵ at 7 °C and two at 50 °C. The average and standard deviation of all four values are listed in Table I, together with values from the literature.[23,26,27] The present results are consistent with high-quality data from the literature.

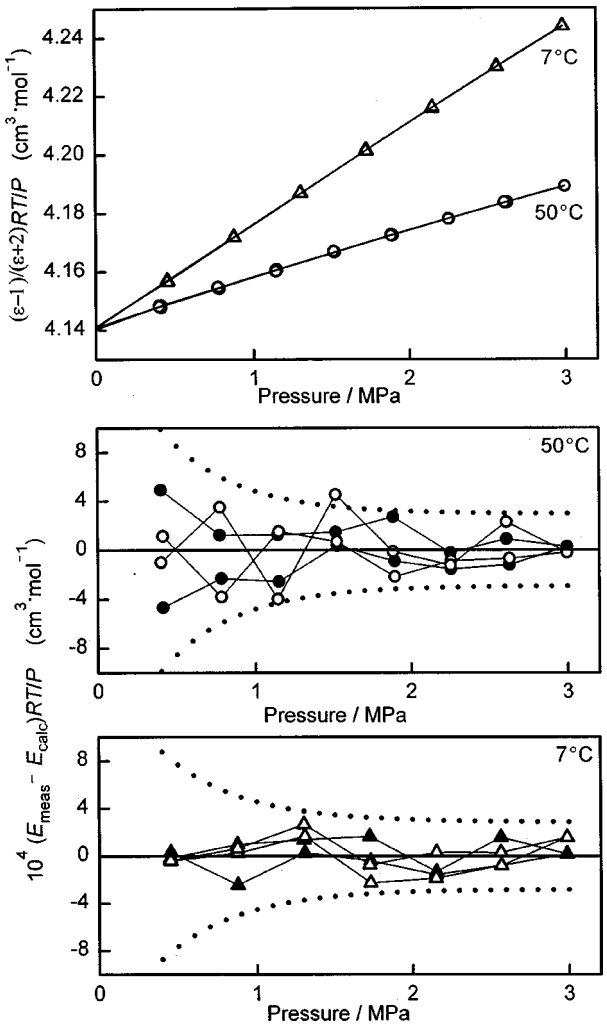

FIG. 6. Polarizability of argon on two isotherms. The top panel shows the pressure and temperature dependence of the data and the quadratic polynomials fitted to them. The lower two panels display the deviations of the data from the polynomials. The dotted curves are the weights used in the fitting. The abbreviation $E\equiv(\epsilon-1)/(\epsilon+2)$ is used in labeling the ordinate.

V. LESSONS LEARNED AND PROSPECTS

In the text above, we mentioned several problems that we encountered with earlier versions of the apparatus. Perhaps others can learn from our experience. An additional concern is that superinvar may not be a satisfactory material for the proposed[7] pressure standard based on capacitance measurements. It was not possible to use RUS to measure the elastic constants of superinvar samples removed from the completed electrodes. An essential requirement for the proposed standard[7] is that the elastic constants be measured accurately. The creep of C_{2x} is also a concern. The proposed pressure standard would be used near 0 °C where there are no reports of unusual creep; however, the standard would have to be baked out at a much higher temperature to prevent the contamination of the test gas.

In the immediate future, the cross capacitors will be installed in new pressure vessels that will be useful up to 10 MPa. Then, the cross capacitors will be entirely satisfactory for determining reference values of the molar polarizability of argon, methane, and similar gases. In turn, the reference

values will be suitable for calibrating the pressure dependence of other capacitors that have a less predictable deformation but are easier to use because they are more compact and have larger capacitances.

ACKNOWLEDGMENTS

The authors thank John Q. Shields and Anne-Marie Jeffery of NIST for their advice, especially concerning cross capacitors and bridges. The authors also thank Dr. Albert Migliori of Los Alamos National Laboratory for measuring the elastic constants of the superinvar samples.

[1] B. A. Younglove and G. C. Straty, Rev. Sci. Instrum. **41**, 1087 (1970).
[2] D. Gugan and G. W. Michael, Metrologia **16**, 149 (1980).
[3] D. P. Fernandez, A. R. H. Goodwin, and J. M. H. Levelt Sengers, Int. J. Thermophys. **16**, 929 (1995).
[4] D. G. Lampard, Proc. IEE, Monograph H. 216M **104C**, 271 (1957).
[5] J. Q. Shields, IEEE Trans. Instrum. Meas. **IM-21**, 365 (1972).
[6] H. Luther, K. Grohmann, and B. Fellmuth, Metrologia **33**, 341 (1996).
[7] M. R. Moldover, J. Res. Natl. Inst. Stand. Technol. **103**, 167 (1998).
[8] A. M. Thompson and D. G. Lampard, Nature (London) **177**, 888 (1956).
[9] J. Q. Shields, R. F. Dziuba, and H. P. Layer, IEEE Trans. Instrum. Meas. **38**, 249 (1989); R. D. Cutkosky, *ibid.* **23**, 305 (1974).
[10] D. Makow, Metrologia **5**, 126 (1969).
[11] J. Q. Shields, IEEE Trans. Instrum. Meas. **IM-27**, 464 (1978).
[12] W. C. Heerens, B. Cuperus, and R. Hommes, Delft Prog. Rep. **4**, 67 (1979).
[13] E. S. Burnett, J. Appl. Mech. **3**, A136 (1936).
[14] A. D. Buckingham, R. H. Cole, and H. Sutter, J. Chem. Phys. **52**, 5960 (1970).
[15] In order to describe materials and experimental procedures adequately, it is occasionally necessary to identify commercial products by manufacturers; names or label. In no instance does such identification imply endorsement by the National Institute of Standards and Technology, nor does it imply that the particular product or equipment is necessarily the best available for the purpose.
[16] D. Makow and J. B. Campbell, Metrologia **8**, 148 (1972); J. B. Campbell and D. Makow, J. Comput. Phys. **12**, 137 (1973).
[17] A. Migliori and J. L. Sarro, *Resonant Ultrasound Spectroscopy* (Wiley, New York, 1997).
[18] S. F. Jacobs, S. C. Johnston, and D. E. Schway, Appl. Opt. **23**, 3500 (1984).
[19] J. W. Berthold III, S. F. Jacobs, and M. A. Norton, Metrologia **13**, 9 (1977).
[20] S. F. Jacobs, S. C. Johnston, and D. E. Schway, Appl. Opt. **23**, 3500 (1984).
[21] J. J. Hurly and M. R. Moldover, J. Res. Natl. Inst. Stand. Technol. (in press).
[22] G. S. Kell, G. E. McLaurin, and E. Whalley, J. Chem. Phys. **68**, 2199 (1978).
[23] J. Huot and T. K. Bose, J. Chem. Phys. **95**, 2683 (1991).
[24] H. R. Orcott and R. A. Cole, J. Chem. Phys. **46**, 697 (1967).
[25] K. Szalewicz, University of Delaware (private communication).
[26] D. Vidal and M. Lallemand, J. Chem. Phys. **64**, 4293 (1976).
[27] A. R. H. Goodwin, J. B. Mehl, and M. R. Moldover, Rev. Sci. Instrum. **67**, 4294 (1996).